INTERNATIONAL ATOMIC ENERGY AGENCY
UNITED NATIONS EDUCATIONAL, SCIENTIFIC AND CULTURAL ORGANIZATION
INTERNATIONAL CENTRE FOR THEORETICAL PHYSICS
I.C.T.P., P.O. BOX 586, 34100 TRIESTE, ITALY, CABLE: CENTRATOM TRIESTE

H4-SMR 393/54

# SPRING COLLEGE ON PLASMA PHYSICS

15 May - 9 June 1989

# PARAMETRIC PROCESSES IN PLASMA (IV)

K. Nishikawa

Hiroshima University
1-1-89 Higashisends-Machi
Naka-Ku
Hiroshima 730
Japan

# Parametric Processes in Plasma IV

## Some Applications to Fusion Research

### 1. Parametric Effects on Lower Hybrid Current Drive (LHCD) in Tokamaks

Lower hybrid wave (slow wave)

$\omega_{ce} \gg \omega \gg \omega_{ci}$

resonance at $\omega^2 = \omega_{LH}^2 = \omega_{pi}^2 / [1 + \omega_{pe}^2/\omega_{ce}^2]$

near resonance : $\omega^2 = \omega_{LH}^2 \left[1 + \frac{m_i}{m_e}\cos^2\theta\right]$ (cold plasma)

away from resonance : ($\omega_{pe}^2 \gg \omega^2 \gg \omega_{LH}^2$)

$$\left(\frac{ck_\perp}{\omega}\right)^2 = N_\perp^2 \doteq \frac{\omega_{pe}^2}{\omega^2}\left[\left(\frac{ck_\parallel}{\omega}\right)^2 - 1\right] = \frac{\omega_{pe}^2}{\omega^2}\left[N_\parallel^2 - 1\right]$$

accessibility : $N_\parallel > N_{acc}$

current generated by suprathermal electrons :

$v_\parallel \sim \omega/k_\parallel \gg v_{Te}$

Two fundamental puzzles :

i) spectral gap : $\left[\frac{\omega}{k_\parallel}\right]_{min} \gg v_{Te}$ at initial plasma

ii) density limit : efficiency $\eta$ drops at high $n_0$

Possible interpretations by parametric effects

i) JIPPT-IIU Ohkubo etal. Nucl. Fusion Lett. 25 (1985) p732-735

ii) F.T. etc. Alladio et al. 12th IAEA Conf. (London, 1984) IAEA-CN-44



Weak dipde pump approximation :

$\omega_0 \gg \omega_{pi}, \omega_{ci}$ .. neglect ion response

$$\frac{1}{\chi_i(\omega)} + \frac{\varepsilon_0}{\varepsilon_e(\omega)} + \frac{\varepsilon_0}{4}\mu^2\left[\frac{1}{\varepsilon_e(\omega+\omega_0)} + \frac{1}{\varepsilon_e(\omega-\omega_0)}\right] = 1$$

$$\mu^2 \doteq a_e^2 = \left[\frac{2e}{m_e}\right]^2 \left\{\left[\frac{k_\perp \cdot E_{0\perp}}{\omega_0^2 - \omega_{ce}^2} + \frac{k_\parallel E_{0\parallel}}{\omega_0^2}\right]^2 + \left[\frac{k_\perp \times E_{0\perp}}{\omega_0^2 - \omega_{ce}^2}\frac{\omega_{ce}}{\omega_0}\right]^2\right.$$

$$\doteq \left(\frac{2e}{m_e}\right)^2 \left\{\left(\frac{k_\parallel E_{0\parallel}}{\omega_0^2}\right)^2 + \left(\frac{k_\perp \times E_{0\perp}}{\omega_{ce}\omega_0}\right)^2\right\} \qquad (\omega_{ce} \gg \omega_0)$$

[polarization drift] [ExB drift]

important at $\omega_{pe}^2 < \omega_0\omega_{ce}$ [edge] ; important at $\omega_{pe}^2 > \omega_0\omega_{ce}$ [centre]

$$1 \doteq -\frac{\mu^2}{4}\frac{\varepsilon_0^2 \chi_e(k,\omega)\,\chi_i(k,\omega)}{\varepsilon(k,\omega)}\left\{\frac{1}{\varepsilon_e(k,\omega+\omega_0)} + \frac{1}{\varepsilon_e(k,\omega-\omega_0}\right.$$

Include electron collisional damping and density gradient :

$$\chi_e(k,\omega) = \frac{1}{k^2\lambda_{De}^2}\,\frac{1 + \frac{\omega - \omega_{*e} + i\nu}{k_\parallel v_{Te}}\Lambda_0(k_\perp^2\rho_e^2)\,Z\left(\frac{\omega+i\nu}{k_\parallel v_{Te}}\right)}{1 + \frac{i\nu}{k_\parallel v_{Te}}\Lambda_0(k_\perp^2\rho_e^2)\,Z\left(\frac{\omega+i\nu}{k_\parallel v_{Te}}\right)}$$

$$\chi_i(k,\omega) = \frac{1}{k^2\lambda_{Di}^2}\left[1 + \frac{\omega - \omega_{*i}}{k_\parallel v_{Ti}}\sum_{\ell=-s}^{s}\Lambda_\ell(k_\perp^2\rho_i^2)\,Z\left(\frac{\omega - \ell\omega_{ci}}{k_\parallel v_{Ti}}\right.\right.$$

where $\nu$ : electron collision freq.

$$\omega_{*j} = \kappa k_y v_{Tj}^2/\omega_{cj}, \qquad \kappa \equiv \frac{1}{n_0}\frac{dn_0}{dx}$$

$(j = e, i)$

$s$ : 50 ~ 100

Experiments on JIPPT-IIU (seed current)

$R = .93m$, $a = .25m$, $B_t = 12.7\,kG$

initial $H^+$ plasma produced by ECR of freq. 33.5 GHz (ordinary mode)

$T_e \sim 200eV$ $N_{e0} \sim 4 \times 10^{12}/cm^3$

$\omega_0 \rightarrow$ $\omega^-$ + $\omega$

[pump $N_{0\parallel} = 1.5 \sim 5$] [lower sideband $N_\parallel = 5 \sim 80$] [highly damped $\omega \sim k_\parallel v_{Te}$]

$E_{res}$: 10–100 keV $\omega_R^-/k_\parallel \sim 3.5 v_{Te}$ $\sim \ell \omega_{ci}$

$\Downarrow$ $< 5$ keV

seed current and bridge spectral gap

$\Downarrow$

perpendicular ion heating

Numerical Analysis: (1D)

$$T_e(r) = T_{e0}\left[1 - \frac{r^2}{a^2}\right]^2 \quad \left(r < \frac{4}{5}a\right)$$

$$n_e(r) = n_e(0)\left[1 - \frac{r^2}{a^2}\right] \quad \left(r < \frac{7}{8}a\right)$$

smoothly connect to measured edge values

$E_{0\parallel}, E_{0\perp}$: use WKB

power flow conservation law with accessibility

Neglect upper sideband: $\varepsilon(\omega + \omega_0)^{-1} = 0$

Given $k_{0\parallel}$, $k_\parallel$ → vary $k_\perp$ and calculate $\omega_R$, $\gamma$



Nucl. Fusion 25 (1985) P733

Ohkubo et al.

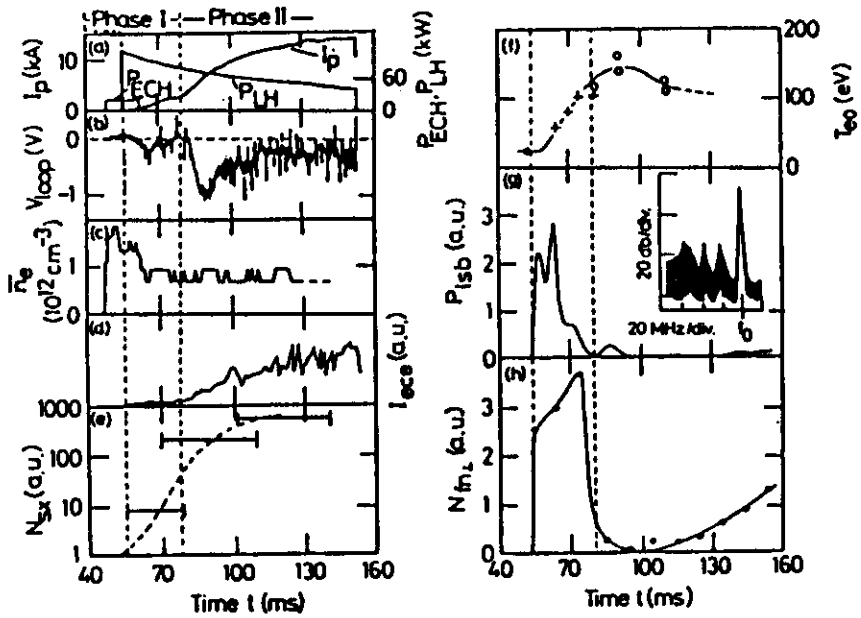


*FIG.1. Time evolution of (a) ECH and RF power, $P_{ECH}$ and $P_{LH}$, and plasma current, $I_p$; (b) loop voltage; (c) line-averaged plasma density; (d) microwave emission near the second electron cyclotron harmonic $I_{ece}$; (e) counts of soft X-rays at an energy of 5 keV; (f) central electron temperature measured by a floating double probe (●), the intensity ratio of the oxygen line (+), and Thomson scattering (○); (g) lower side-band power at $f = 700$ MHz received by the RF probe, and frequency spectrum; (h) counts of fast neutral particles measured perpendicularly at an energy of 1.8 keV.*

Nucl. Fusion 25 (1985) p734
by Ohkubo et al.

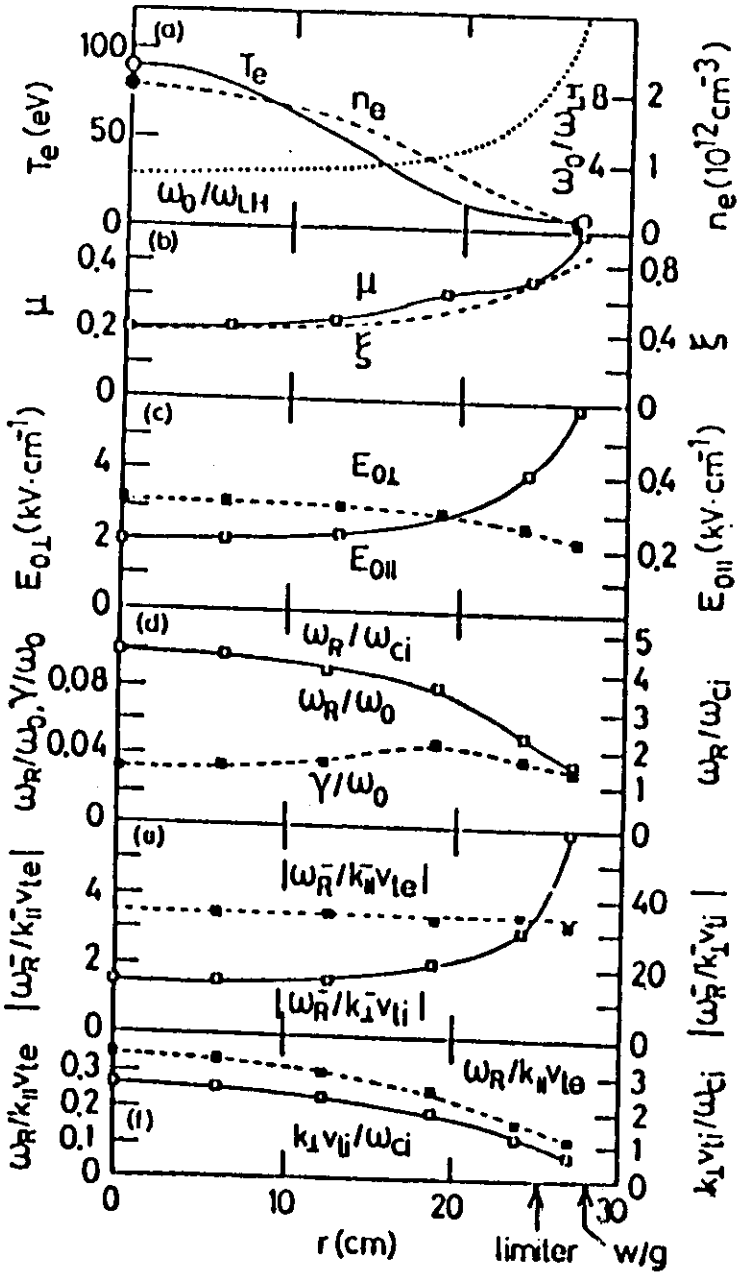


Nucl. Fusion 25 (1985) p734
by Ohkubo et al.

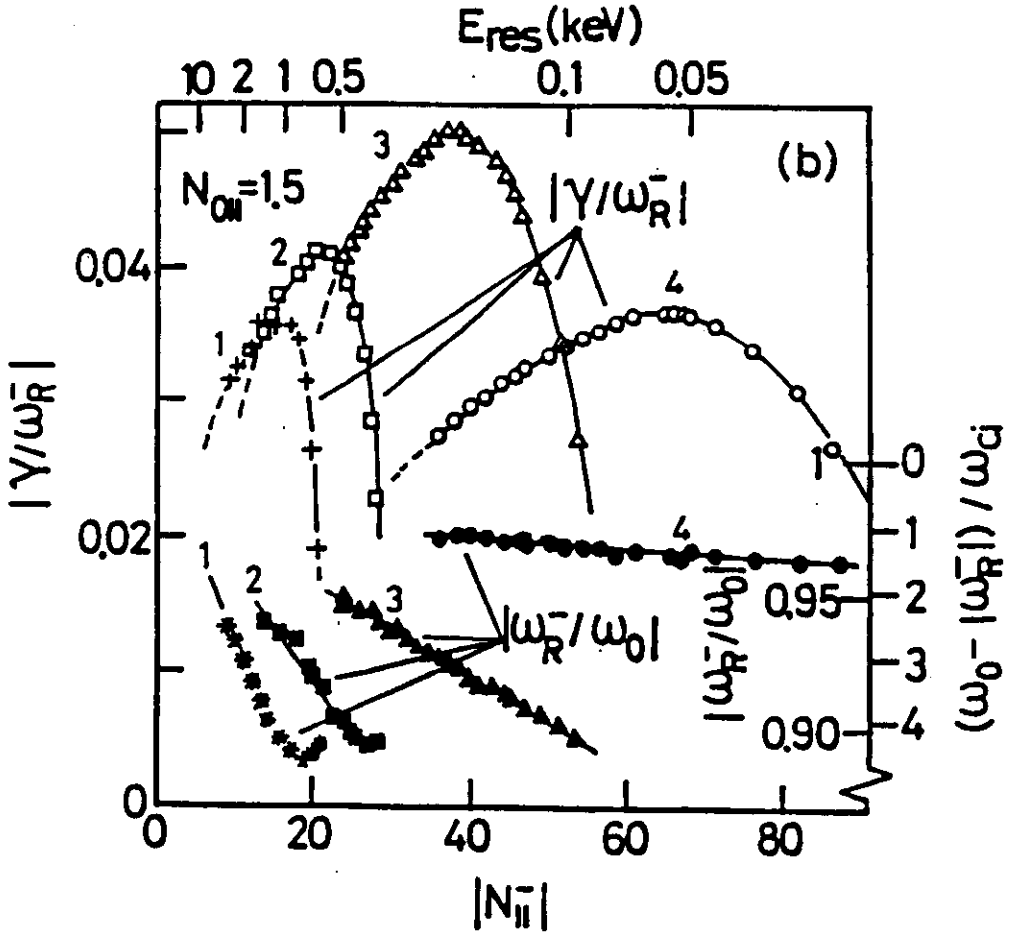

F. T. Tokamak

$B_t = 80\,kG$, $n_o = 3 \sim 17 \times 10^{13}/cm^3$

$P_{OH} \sim 500\,kW$ ($I_p \sim 350\,kA$)

$P_{ad.} \lesssim 300\,kW$ (L.H.H. at 24 GHz, $N_{\parallel} = 1.3 \sim 2.5$) (upshifted to ~7)

$\Delta T_e \sim 700\,eV$, $D^+ + H^+$ (minority $\lesssim 3\%$)

Low density $n_o < 5 \times 10^{13}/cm^3$

strong electron heating measured by ECE emission

Intermediate density $5 \times 10^{13} < n_o < 15 \times 10^{13}/cm^3$

$H^+$ tail heating and parametric decay instability

High density $n_o > 15 \times 10^{13}/cm^3$

ion tail heating drops by parametric instability at edge, inhibiting wave propagation to centre.

$n_{critical}$ insensitive to $\omega/\omega_{LH}$, $\omega_{pe}/\omega_{ce}$ and $\bar{n}^{-1}$, $m_i$, or kinetic effects.

XIIth IAEA Conf. (Sept. 1984, London) IAEA-CN-44/F-I-3

b, Alladio et al.

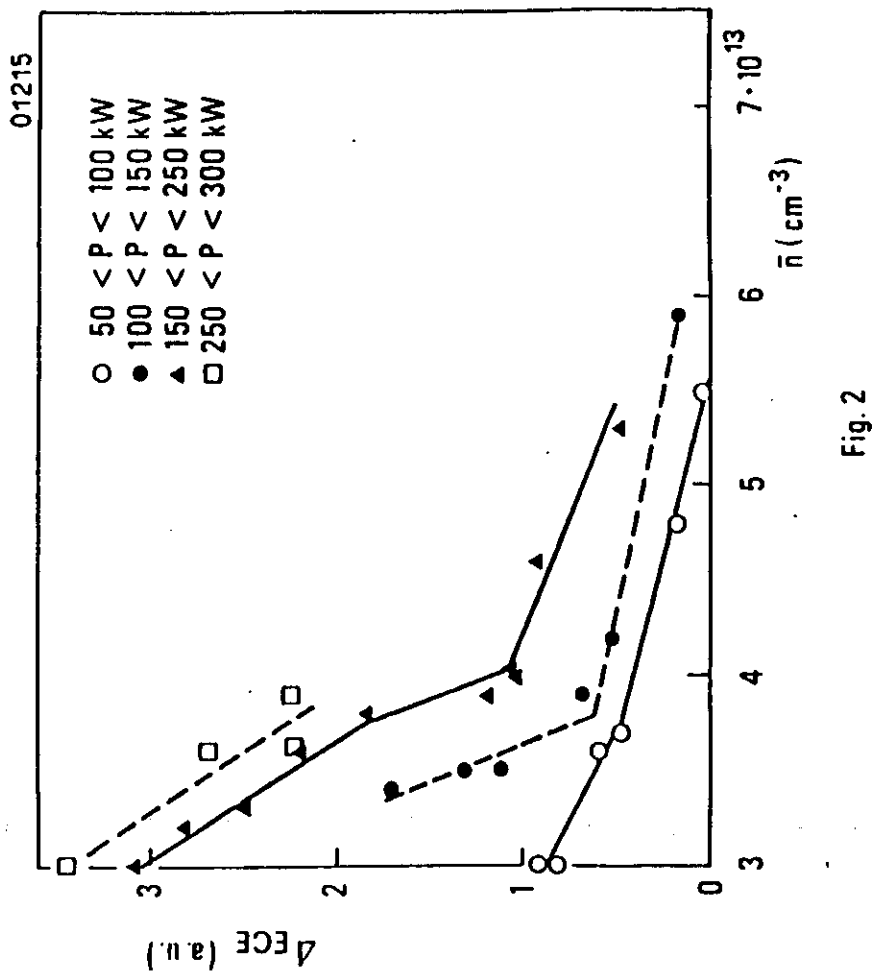


Fig. 2

XVth IAEA Conf. (1984, London) IAEA-CN-44/F-J-3
by Alladio et al.

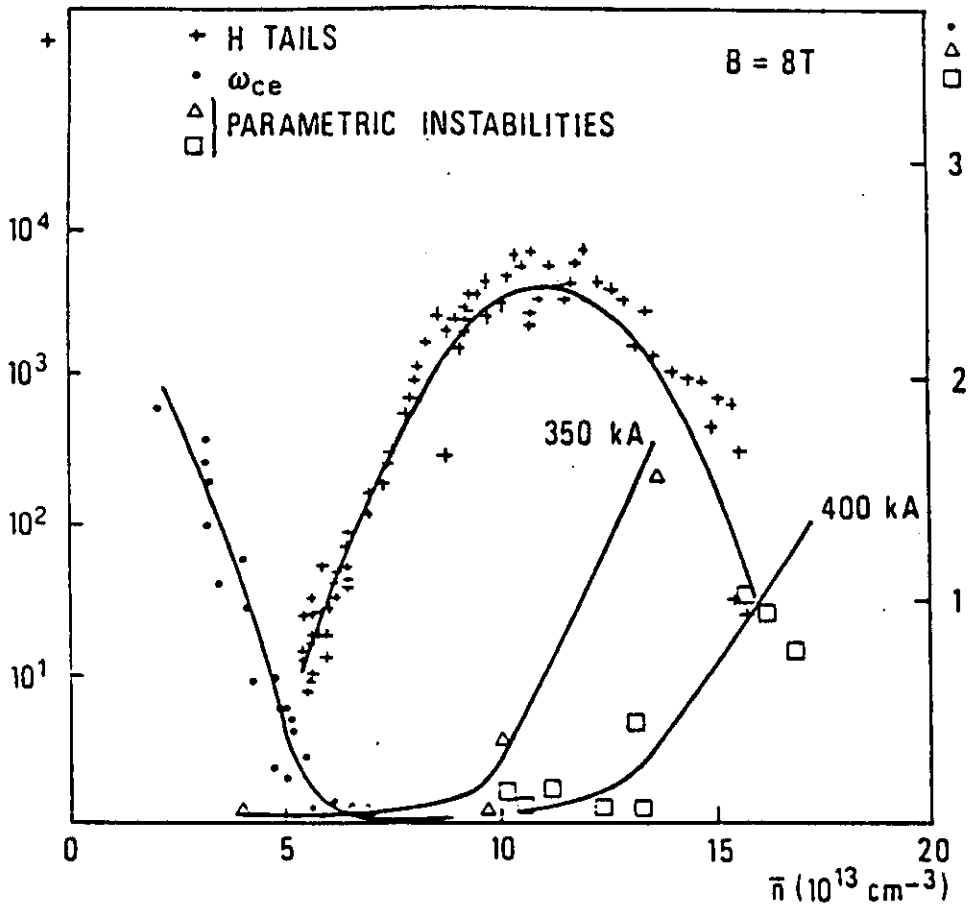


Fig. 1



## 2. Stimulated Raman scattering (SRS) in laser produced plasmas.

SRS backscattering can take place in the region $0 < n_0 < n_c/4$, where $n_c$: critical density ($\omega_0 = \omega_{pe}$)

Convective in presence of $L = \left(\frac{1}{n_0}\frac{dn_0}{dx}\right)^{-1}$

Amplitude $I_{SRS}$ determined by Rosenbluth amplification factor:

$$I_{SRS} = I_{noise} \exp\left[2\pi\gamma^2 / |\kappa' v_{gSRS} v_{gepw}|\right]$$

where $\gamma^2 = \frac{k^2 v_0^2}{8 k_0 c}\omega_{pe} \doteq \frac{k_0 v_0^2}{2c}\omega_{pe}$

$$|\kappa'| \doteq \left|\frac{dk(x)}{dx}\right| \doteq \frac{1}{3k\lambda_D^2}\frac{1}{L} = \frac{1}{6k_0\lambda_D^2}\frac{1}{L}$$

$$\left(\text{cf. } k^2(x) - k^2(0) \doteq \frac{\omega_{pe}^2}{3V_{Te}^2}\frac{x}{L} = \frac{1}{3\lambda_D^2}\frac{x}{L}\right)$$

$v_{gSRS} \doteq c \qquad v_{gepw} \doteq 3k\lambda_D V_{Te} = 6k_0\lambda_D V_1$

$$\therefore \frac{2\pi\gamma^2}{|\kappa' v_{gSRS} v_{gepw}|} = \pi E \frac{v_0^2}{c^2} k_0 L > 1$$

[threshold]

<u>SRS important for large target</u> where L large.

Cause { · <u>reflection</u> (cf Manley-Rowe relation)
· <u>hot electron production</u> by epw Landau damping → core preheating.

## Experimental results

(both for overdense and for underdense targets)

i) Growth characteristics.
   threshold ..... very low
   intensity ..... very high  etc.

ii) "Raman gap"
   observed only in $0.01\, n_c < n_0 < 0.05\, n_c$
   (Baldis et al. $CO_2$ laser on underdense plasmas)

Possible interpretations

i) hot spots, filamentation, ripples, turbulence etc.
   noise enhancement by e-beam generated at $n_0 = n_c/4$.
   (Simon et al.)
   coupling of forward Raman and backward Raman ⇨ absolute instability
   (Koch-Williams, Barr et al., Villeneuve et al.)

ii) low density limit
   due to Landau damping of epw ($\omega \gg \omega_{pe}$)

   high density limit:
   coupling to SBS or ion density fluctuation
   ⇨ detuning of SRS (Walsh et al.)
   Langmuir collapse and cavitan formation
   ⇨ seed SBS (Aldrich et al., Rose et al.)
   Rosmus et al.

R.P. Drake et al. Phys. Rev. Lett. 60 (1988) 1018
Fig. 3

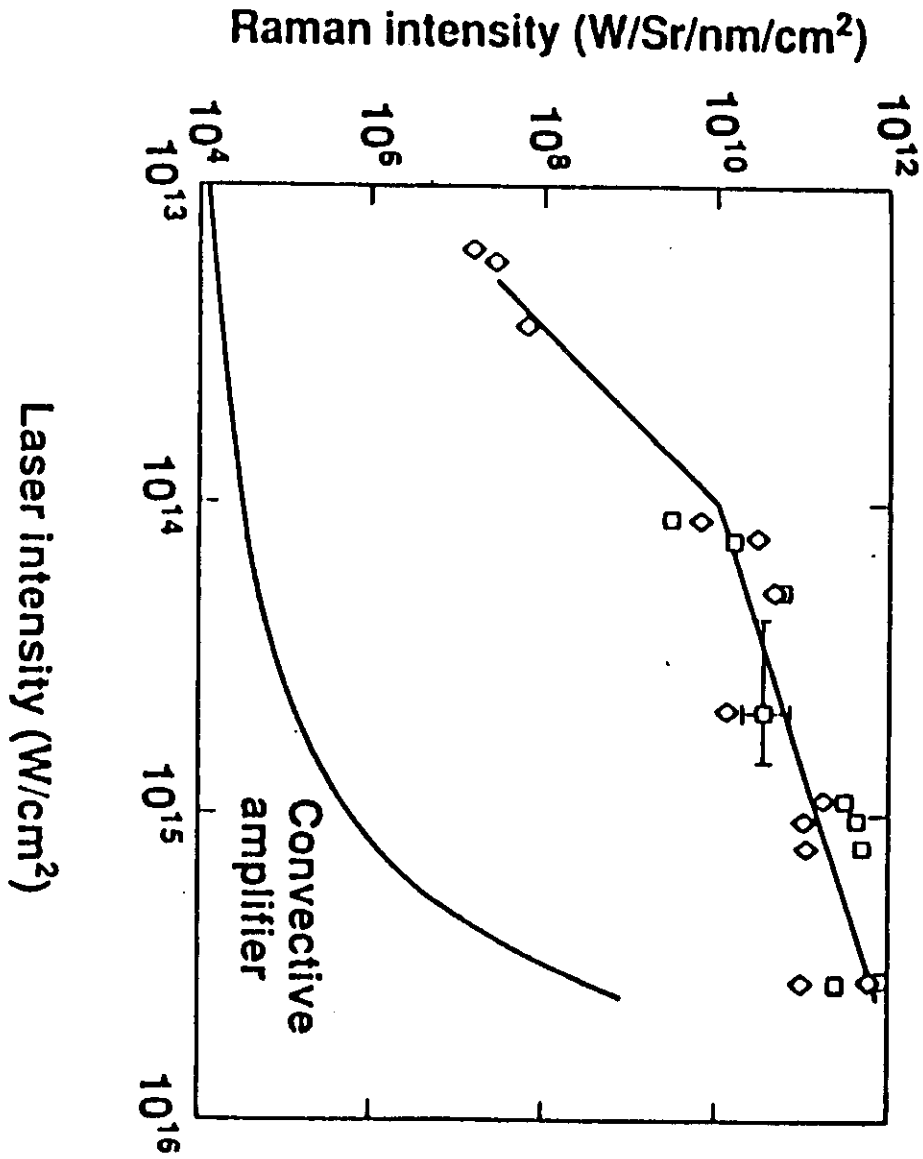

# Coupling of forward Raman and backward Raman

Resonance conditions $\begin{cases} \text{Let } k_s \neq k_0 \\ \end{cases}$ $\begin{cases} k_0 = k + k_s \text{ or } k = k_0 - k_s \perp k_0 \\ \text{(forward scattering)} \\ k_0 = k - k_s \text{ or } k = k_0 + k_s \simeq 2k_0 \\ \text{(back scattering)} \end{cases}$

with $\omega_0 = \omega_s + \omega_k$

$$\omega_k^2(x_f) = \omega_p^2(x_f) + 3|k_0 - k_s|^2 v_{Te}^2$$

$$\omega_k^2(x_b) = \omega_p^2(x_b) + 3|k_0 + k_s|^2 v_{Te}^2$$

$\omega_k(x_f) = \omega_k(x_b)$ when $\omega_p^2(x_b) = \omega_p^2(x_f) - 12 k_0 \cdot k_s v_{Te}^2$

If $\omega_p^2(x_b) = \omega_p^2(x_f)\left[1 - \frac{x_b - x_f}{L}\right]$

$$\rightarrow x_b - x_f = 12 k_0 \cdot k_s \lambda_{Df}^2 L$$

If $\omega_p^2(x_b)\left[1 - \left(\frac{x_b - x_f}{L}\right)^2\right]$

$$\rightarrow x_b - x_f = 2\sqrt{3}\,[k_0 \cdot k_s]^{1/2} \lambda_{Df} L$$

Koch-Williams: Feedback loop

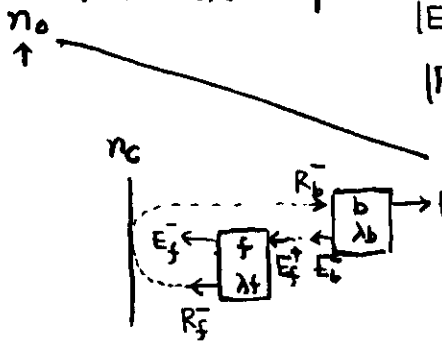


$$|E_f^-|^2 = |E_f^+|^2 e^{2\pi\lambda_f}$$

$$|R_f^-|^2 = |E_f^-|^2 - |E_f^+|^2 = \left(e^{2\pi\lambda_f} - 1\right)|E_f^+|^2$$

$$|E_f^+|^2 = |E_b^-|^2 e^{-2D_e}$$

$$|R_b^-|^2 = |R_f^-|^2 = e^{-2D_R}$$

$$|R_b^+|^2 = |R_b^-|^2 e^{2\pi\lambda_b}$$

$$|E_b^-|^2 = |R_b^+|^2 - |R_b^-|^2 = \left(e^{2\pi\lambda_b} - 1\right)|R_b^-|^2$$

$$\left|\frac{E_b^-}{R_f^-}\right|^2 e^{-2D_e} \left|\frac{R_f^-}{E_i^+}\right|^2 e^{-2D_R} = 1 \Rightarrow \left(e^{2\pi\lambda_f} - 1\right)\left(e^{2\pi\lambda_b} - 1\right) = e^{2(D_e + D_R)}$$

[dispersion relation]

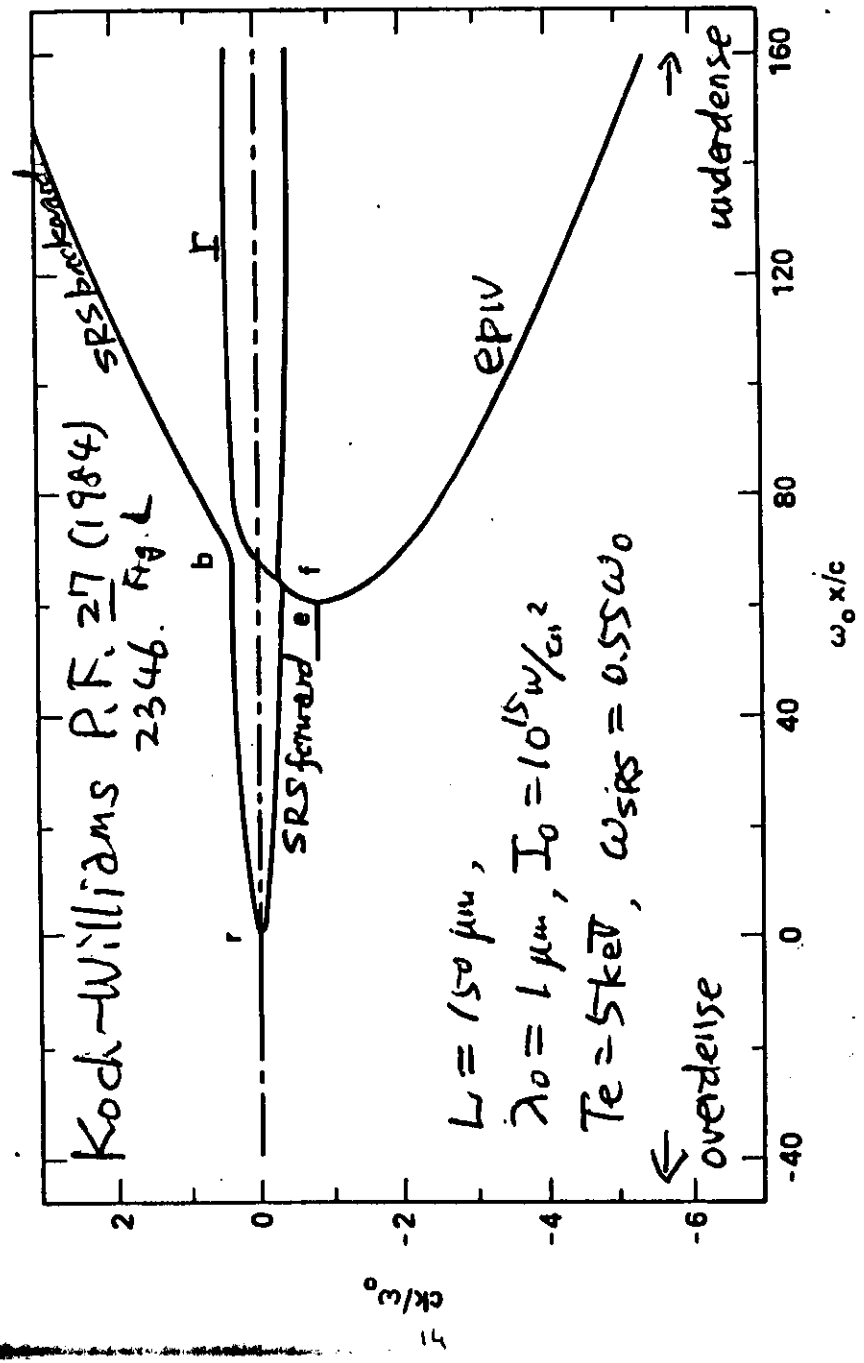

Growth rate (absolute instability)

$$\gamma = \pi \left[\frac{V_0^2 \omega_p^2}{3 V_T^2 c^2}\right] \frac{k_0 \omega_p^2}{8 x' \omega_0 k_s^2 L} \left[1 + \frac{k_s^2}{k_0^2 - k_s^2}\right]$$

Numerical analysis by Bair et al.

Solved $\left[\frac{\partial^2}{\partial t^2} + \omega_p^2(x) - \frac{\partial^2}{\partial x^2}\right] V_s = V_0 \frac{\partial E_p}{\partial x}$

$$\left[\frac{\partial^2}{\partial t^2} + \omega_p^2(x) - 3V_{Te}^2 \frac{\partial^2}{\partial x^2}\right] E_p = \omega_p^2(x) \frac{\partial}{\partial x}[V_0 V_s]$$

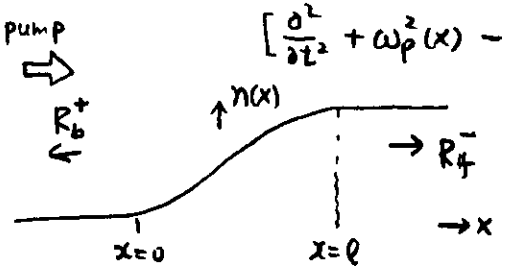


for both absolute and convective case [with noise]

$n_{max} > n_c$ : total reflection of $R_f^-$

$n_{max} < n_c$ : partial transmission of $R_f^-$

⇨ Results agree with Koch-Williams

Experiment by Villeneuve, Baldis

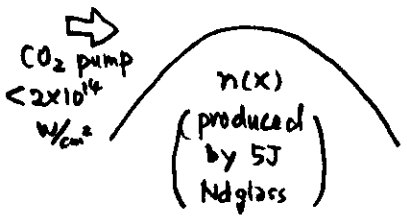


SRS backscatter : absolute

forward scatter : convective

coupling ⟶ absolute for both ?

Theoretical threshold ($T_e$ 500eV, $n_{max} \sim 0.05 n_c$)

$\sim 10^{12}$ W/cm² for b.s.

$\sim 7 \times 10^{13}$ W/cm² for f.s (convective)

SRS observed at early phase below $10^{13}$ W/cm²

H.C. Bair et al Phys. Rev. Lett. 60 (1988) 1950

Fig. 2

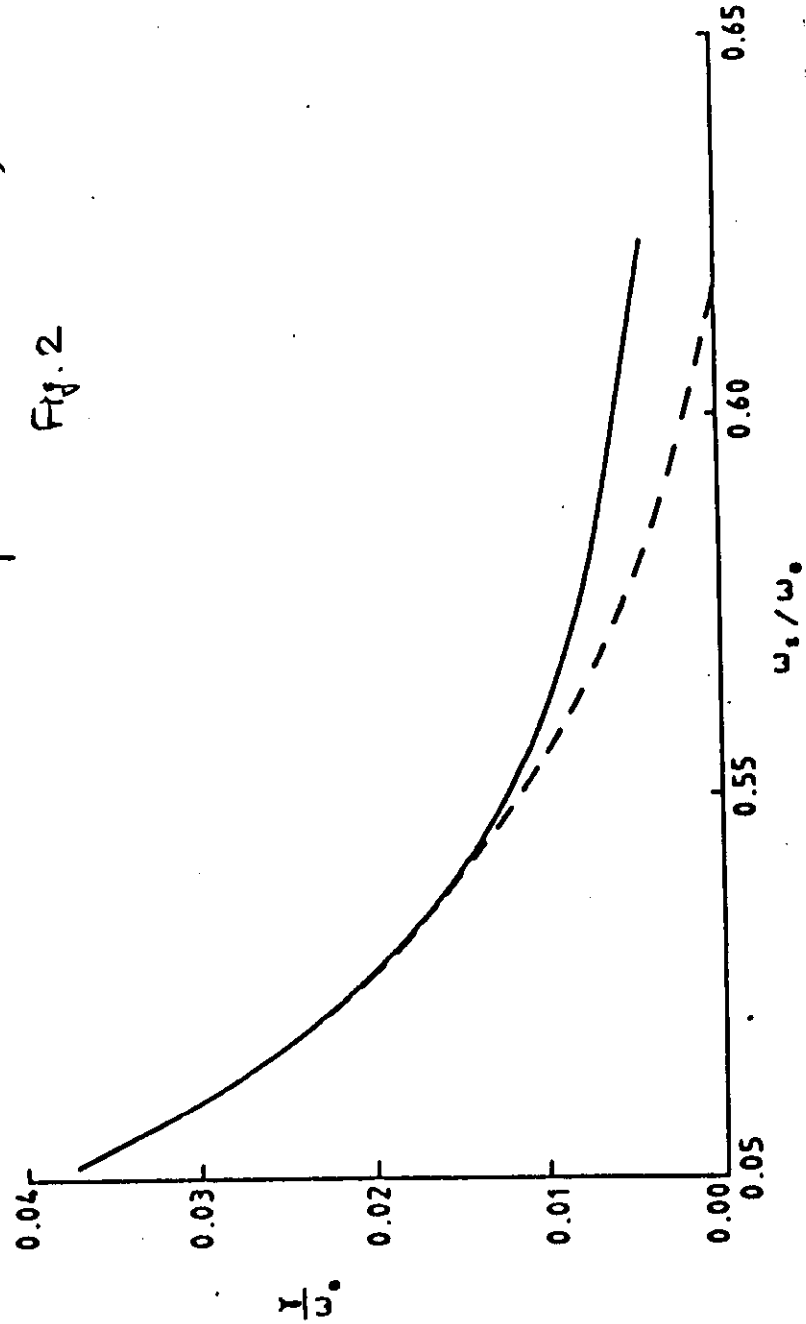

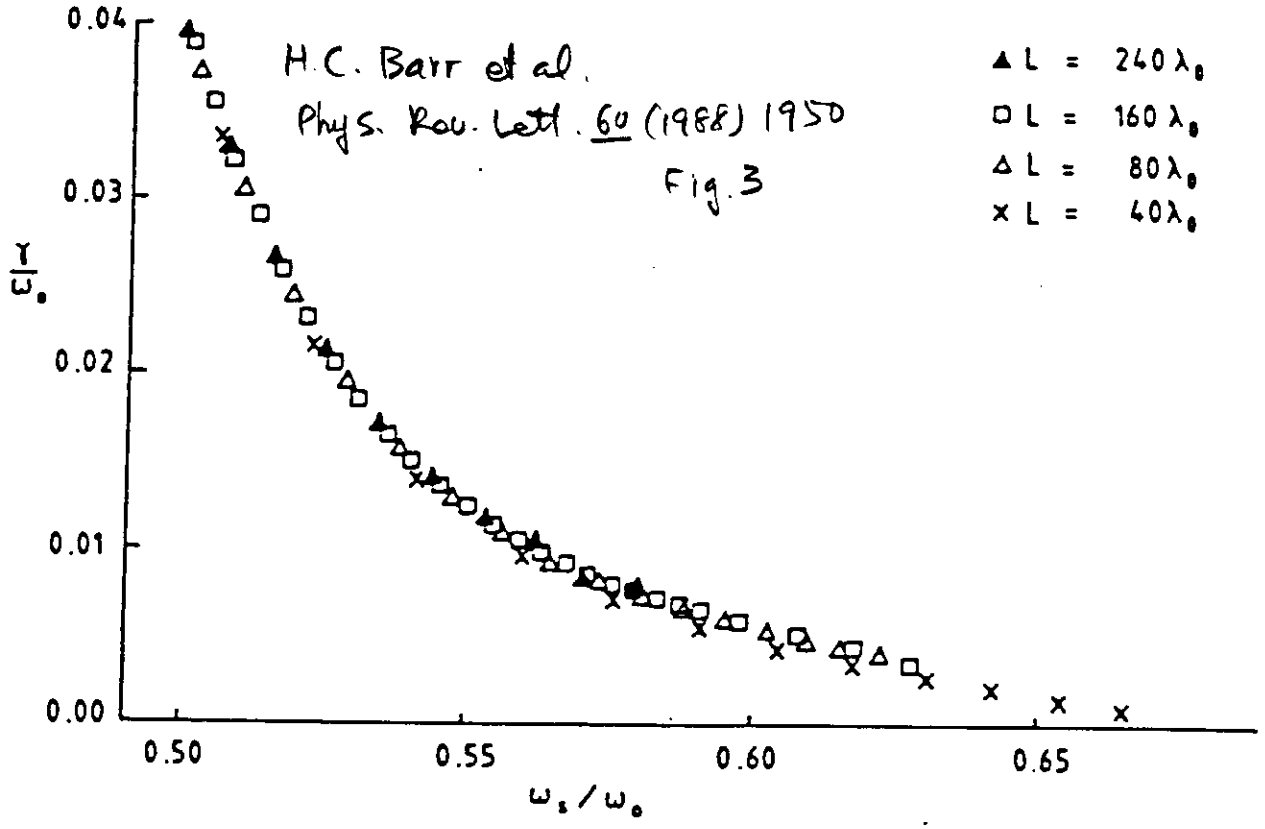


H.C. Barr et al. Phys. Rev. Lett 60 (1988) 1950

Fig. 4

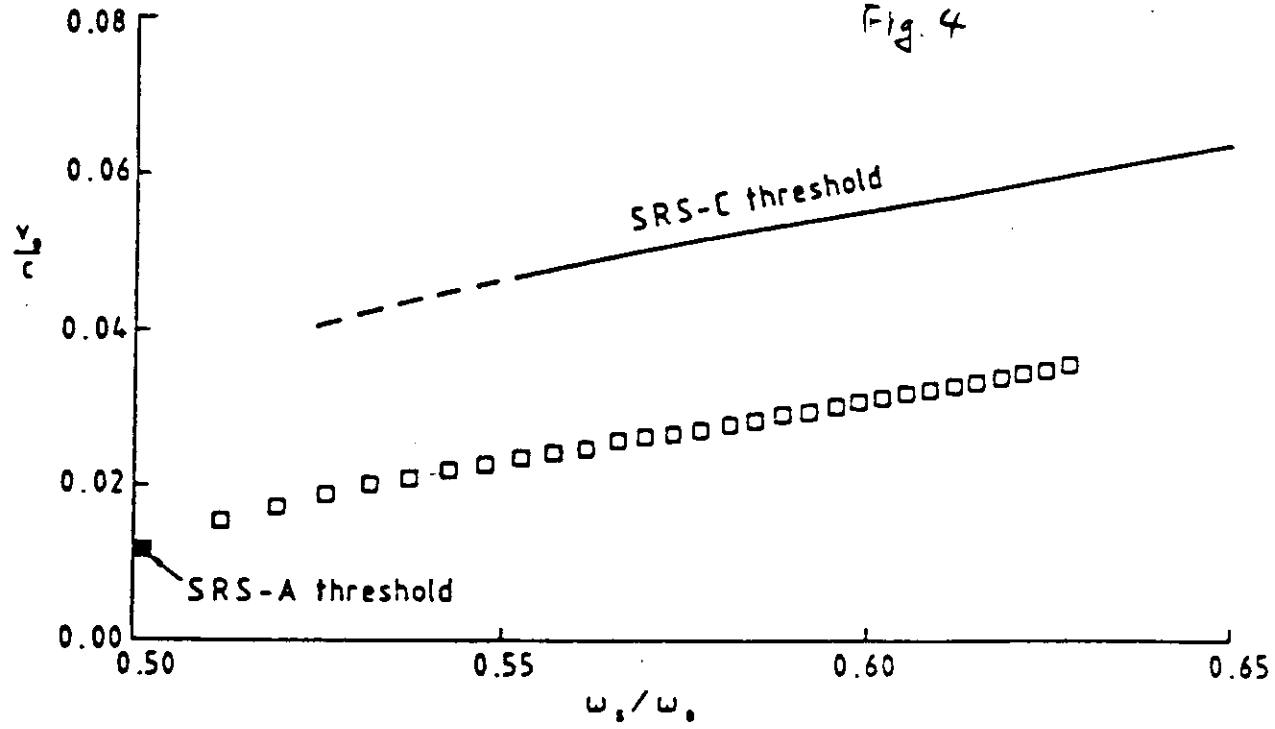

D.M. Villeneuve and H.A. Baldis
Phys. Fluids 31 (1988) 1790 Fig. 1




$I_{back} \times \frac{1}{50} \sim I_{forward}$

D. M. Villeneuve and H. A. Baldis
Phys. Fluids 31 (1988) 1790 Fig. 4

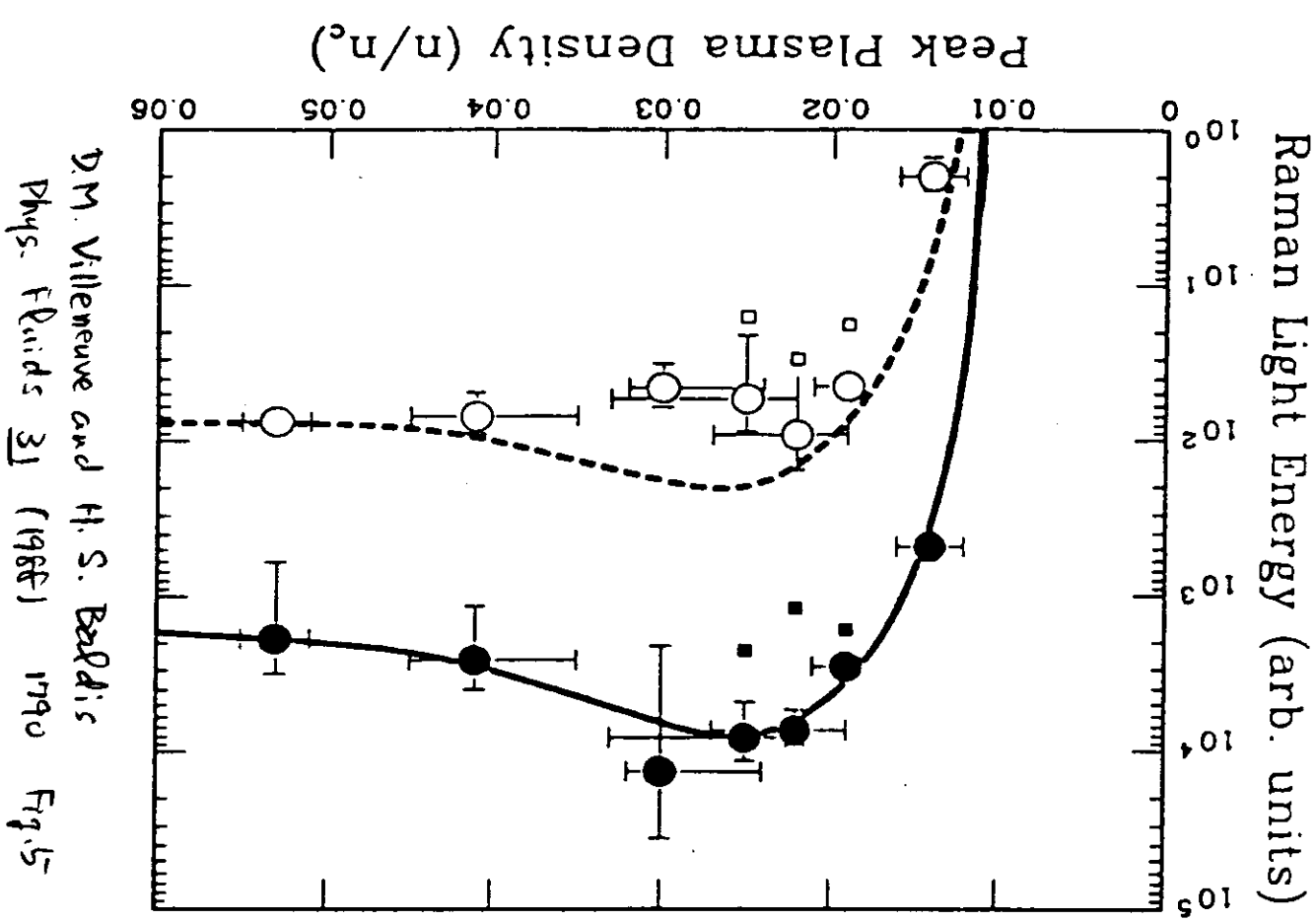


## Experimental evidence of competition between SRS and SBS

### $CO_2$ Experiments:

*(Electron and ion acoustic waves detected by Thomson Scattering)*

A)
- First reported in 1984.
- Quenching of SRS by ion acoustic waves.
- Observations consistent with "*Raman Gap*".

B)
- Total supression of SRS by seeding of an ion wave by means of optical mixing.
- Spatial resolution of electron and ion waves.

### NOVA experiments:

*(Detection of SRS and SBS scattered ligth)*

- Early saturation of SRS when high levels of SBS are present.
- Strong growth of SRS observed *only* after SBS signal drops.

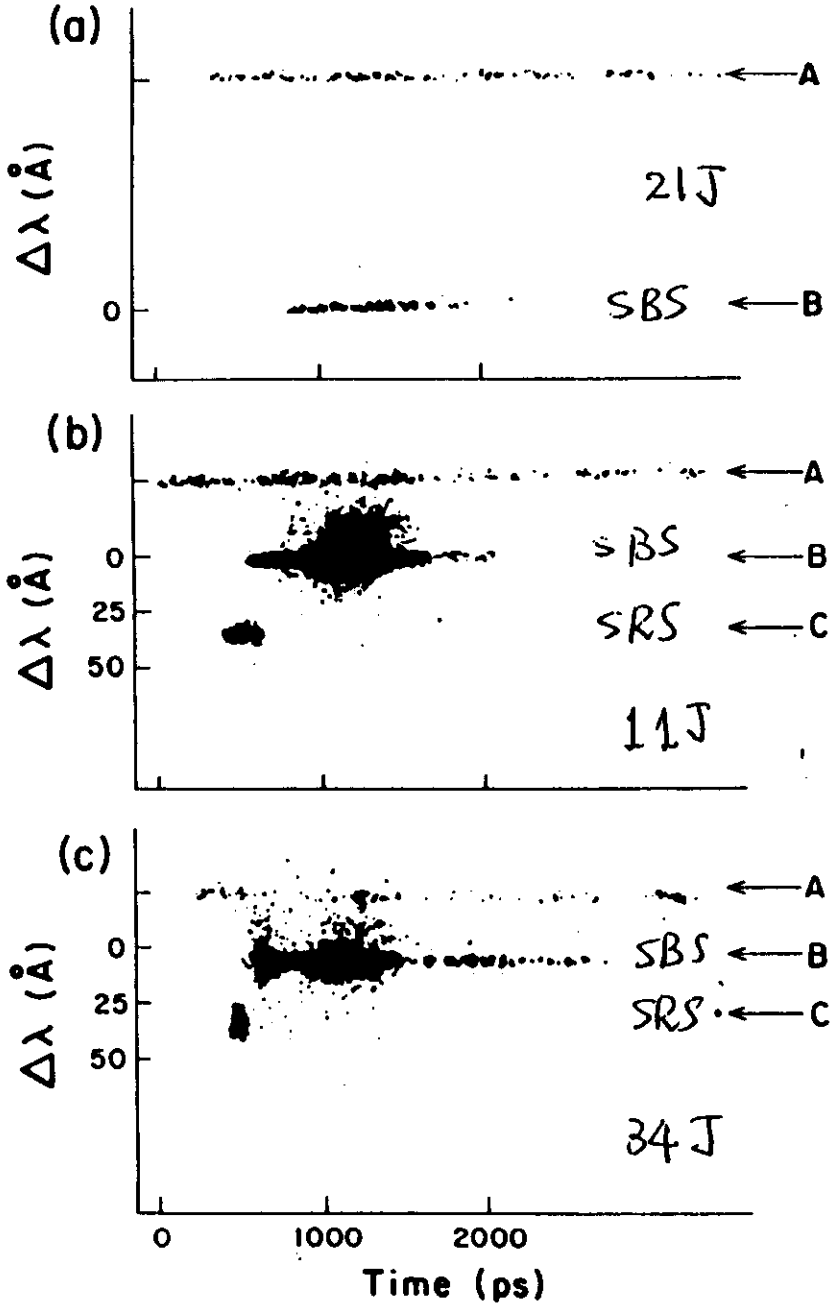


C. J. Walsh et al. Phys. Rev. Lett. 53 (1984) 1445 Fig. 3



## Rose-DuBois-Bezzerides theory

em w: $A^T = \frac{1}{2}\{ A e^{-i\omega_0 t} + c.c. + A_R e^{-i\omega_R t} + c.c. \}$

[pump + SBS] [SRS]

l.f.w: $\frac{1}{2} E e^{-i\omega_p t} + c.c. + n(x,t)$

[epw] [iaw]

Basic eq'ns

$$\{-2i\omega_0 \partial_t + (\omega_p^2 - \omega_0^2) - c^2\partial_x^2\} A = -\omega_p^2 \frac{n}{n_0} A + \frac{e}{2m}\partial_x [E A_R]$$

$$\{-2i\omega_0 \partial_t + (\omega_p^2 - \omega_R^2) - c^2\partial_x^2\} A_R = -\omega_p^2 \frac{n}{n_0} A_R + \frac{e}{2m}\partial_x [E^* A]$$

$$\{-2i\omega_p \partial_t + \omega_p^2 \frac{n}{n_0} - 3V_{Te}^2 \partial_x^2\} E = -\frac{\omega_p^2}{2c^2}\frac{e}{m}\partial_x [A A_R^*] + \delta S_E$$

$$\{\partial_t^2 - C_s^2 \partial_x^2\} n = \frac{1}{4\pi n_i m_i}\partial_x^2 \left\{ |E|^2 + \frac{\omega_p^2}{c^2}[|A|^2 + |A_R|^2] \right\} + \delta S_n$$

where $\delta S_E$, $\delta S_n$ : noise source at $k_E \pm 2k_0$

- effective damping added
- plasma : slab with

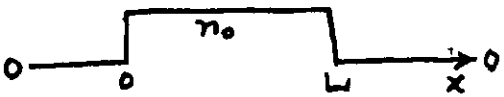


- pump : $A_0 = a_0 e^{ik_0 x}(t/\tau)^{1/2}$ ($\tau = 500$ ps)
- boundary condition : $A_R(x=L)=0$, $A(x=L) = A_0$

E and n outgoing in $x<0$ and $x>L$

⇨ transition density: at $\gamma_R \simeq 2\gamma_B$

i.e. $\gamma_R > 2\gamma_B$ → SRS on, $\gamma_R < 2\gamma_B$ no SRS

SRS → Langmuir collapse → density cavity → enhanced noise

enhanced noise of n → SBS → $dn/dt$ → quench SRS by detuning

$$\frac{dn}{dt} \to \frac{d\Delta\omega}{dt}\gamma_R^{-1} \geq \gamma_R \to \text{suppress SRS.}$$

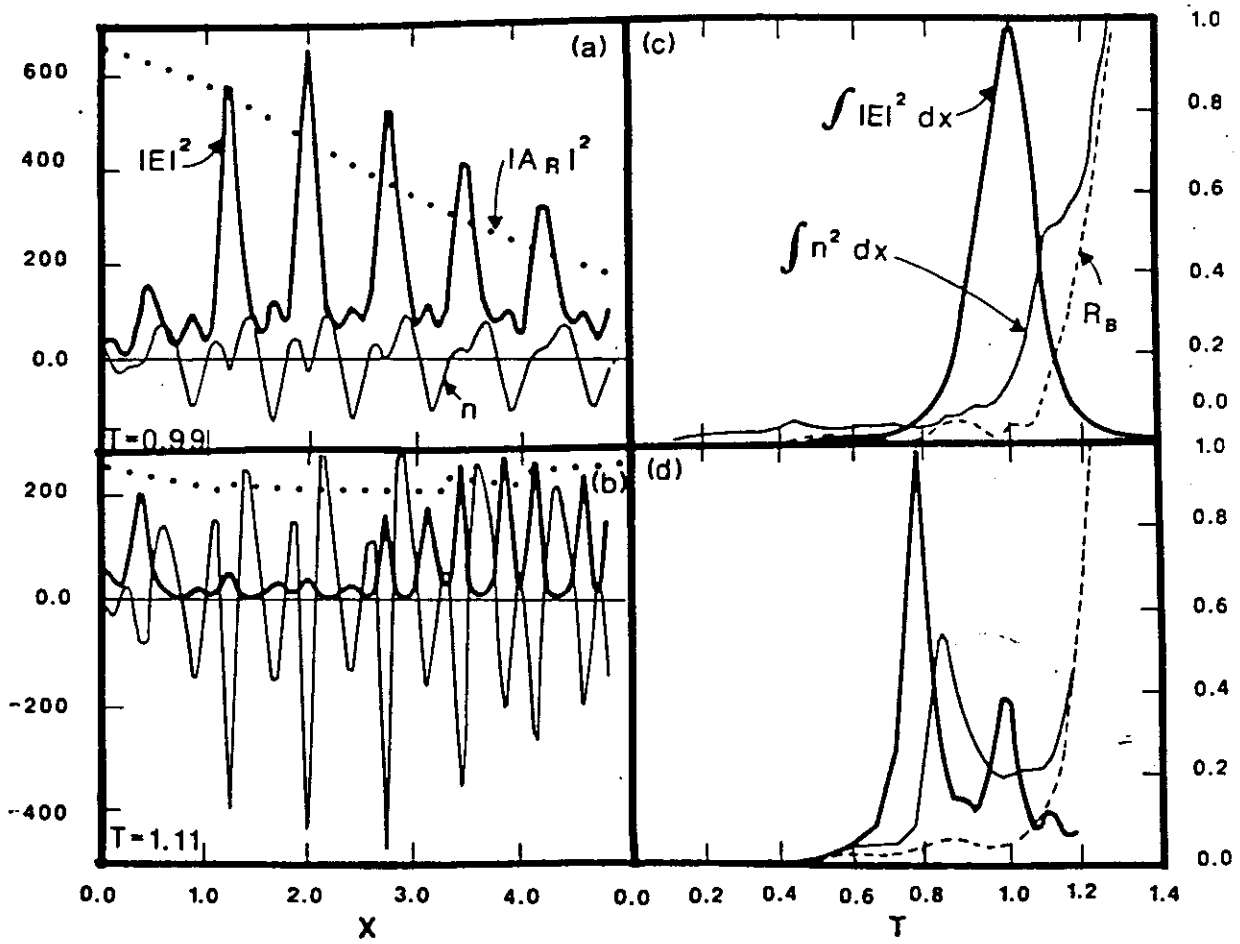


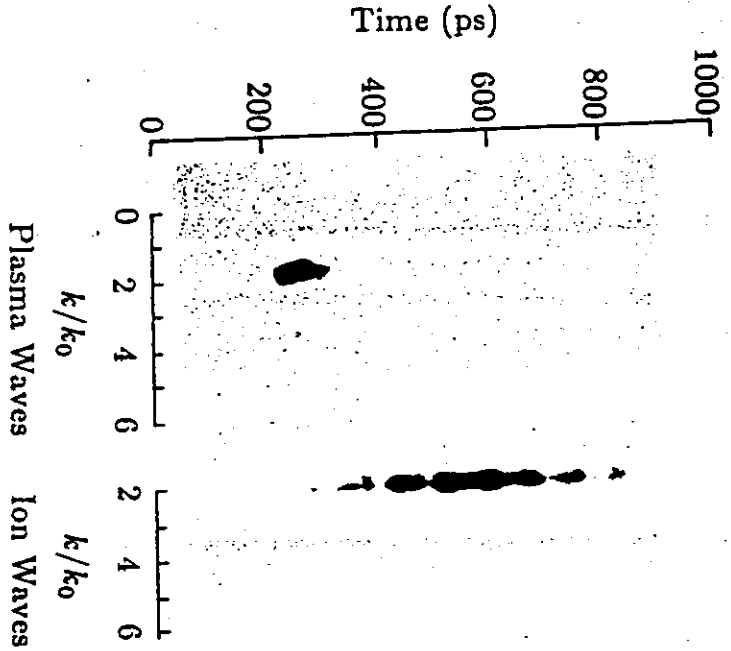


**Streaked k-spectrum of Ion and Plasma Waves**

No seed beam

$n/n_c = 0.035$

87031106

H. A. Rose et al. Phys. Rev. Lett. 58 (1987) 2547 Fig. 2

## Streaked k-spectrum of Ion and Plasma Waves

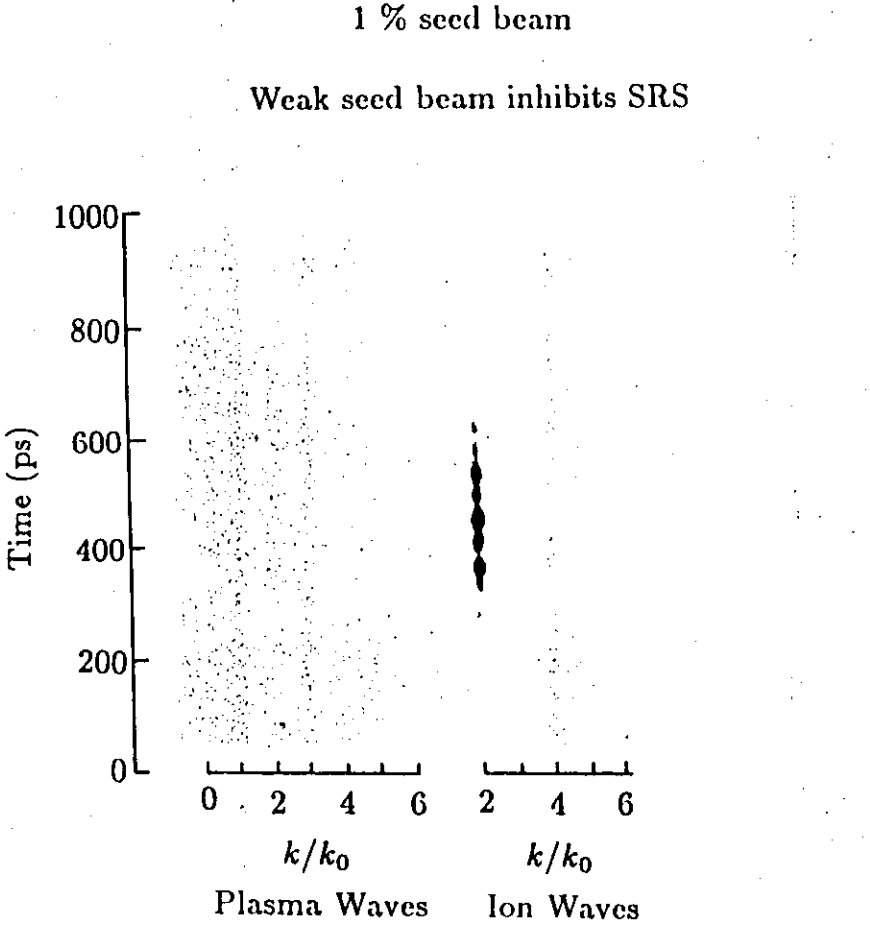


D. M. Villeneuve et al.
Phys. Rev. Lett. 59 (1987) 1585
Fig. 3

87031110



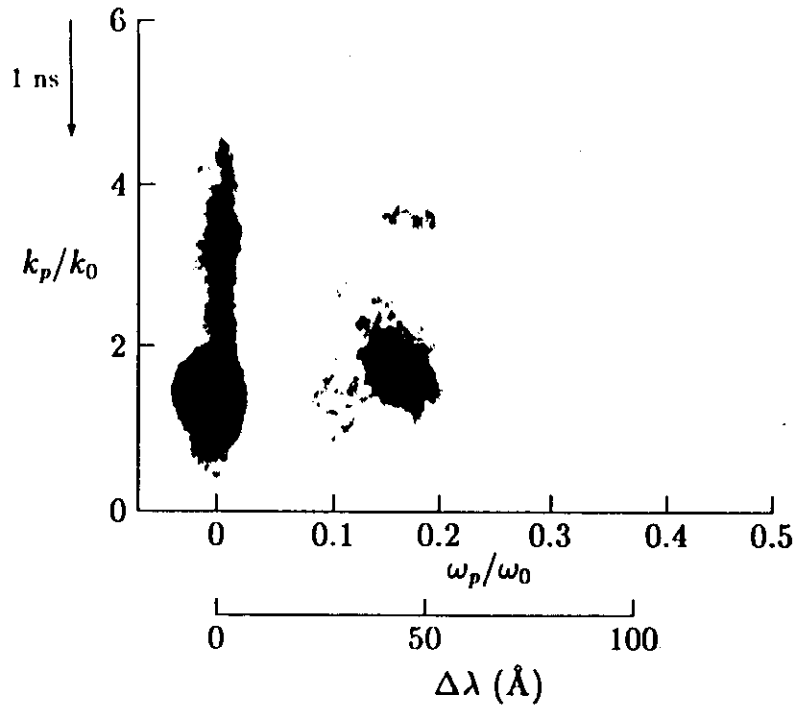


FIG. 4. An $\omega$-$k$ plane image of a shot with a seed beam intensity only $\simeq$0.2% of the pump's. The harmonic $(\omega_p, k_p+2k_0)$ is consistent with coupling with the stronger seeded ion waves, and the lack of frequency harmonics indicates a weaker plasma wave.

D. M. Villeneuve et al.
Phys. Rev. Lett. 59 (1987) 1585

Parametric instabilities

at quarter critical density

$\omega_0 \doteq 2\omega_{pe}$ $\quad n_0 \doteq n_c/4$

- Two plasmon decay (TPD)

$(k_0, \omega_0) \longrightarrow (k_1, \omega_1) + (k_2, \omega_2)$

[pump emw] [epw] [epw]

$k_0 = k_1 + k_2$ , $\omega_0 = \omega_1 + \omega_2$, $\omega_1 \sim \omega_2 \sim \omega_{pe}$

- Absolute Raman

$(k_0, \omega_0) \longrightarrow (k_s, \omega_s) + (k, \omega)$

[pump emw] [SRS emw] [epw]

$k_0 = k_s + k \doteq k$ $\quad \omega_0 = \omega_s + \omega$ , $\omega_s \sim \omega \sim \omega_{pe}$

$(k_s \doteq 0)$

Need to include nonlinearity in continuity eq.

- TPD $\quad \gamma_{max} = \frac{k_0 |v_{01}|}{2} \left[1 - \frac{3\sqrt{3}\, v_{Te}^2}{4\omega_{pe} |v_{01}|} k_y\right] - \Gamma$

where $k_y = k \cdot (k_0 \times E_0)/k_0 E_0$,

$\Gamma$ = damping = $\frac{\omega_{pe}}{4 k_y L}$ for convective damping

at $k_x = \frac{k_0}{2}\left[1 \pm (1 + 4(\frac{k_y}{k_0})^2)^{1/2}\right]$ $\quad (L = (\frac{1}{n_0}\frac{dn_0}{dx})^{-1}$

Secondary instability

$(k_1, \omega_1) \rightarrow (k_2, \omega_2) + (k_1 - k_2, \omega_1 - \omega_2)$

[ion acoustic wave]



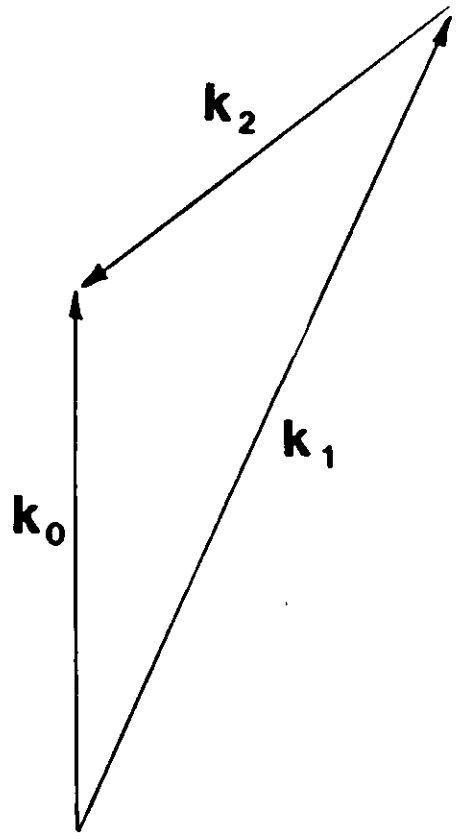


FIG. 4. A representative wave-vector diagram for TPD. $k_0$ is the pump wave, and $k_1$ and $k_2$ are the two daughter waves. A wide range of daughter waves is allowed.

H. A. Baldis et al.
Can. J. Phys. 64 (1986) 961

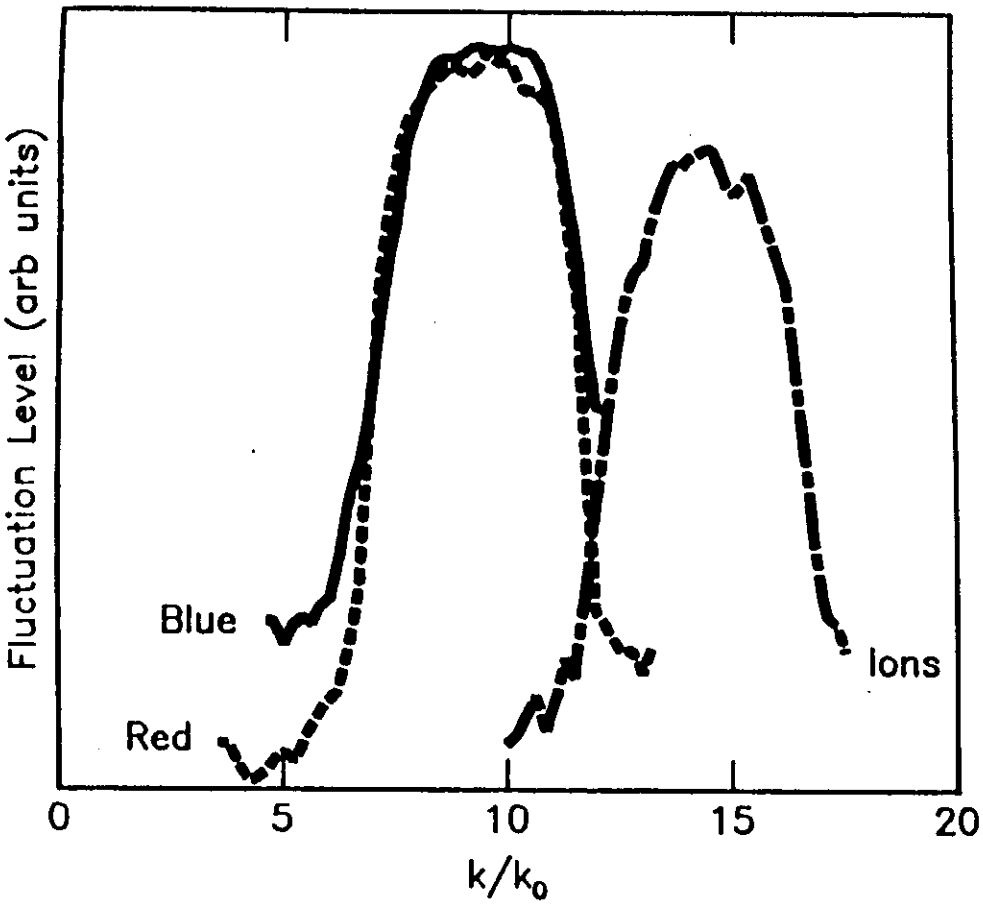


Fig. 3
Spectrum of fluctuations of ion and plasma waves measured from a streak photograph. The "red" and "blue" spectra correspond to plasma waves travelling at approximately 45 and 135° to $k_o$. The ion waves can be travelling along either direction.

H. A. Baldis et al from Laser Interaction and Related Plasma Phenomena Vol 7 (Plenum 1986) 299

## EXAMPLES OF EXPERIMENTAL OBSERVATIONS OF COUPLING BETWEEN PLASMA MODES

Measured growth rate of two-plasmon decay plasma waves and ion waves produced by coupling between plasma waves

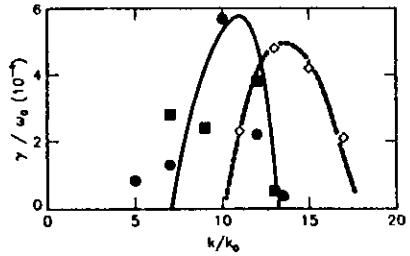


Harmonics of absolute SRS plasma waves produced by coupling with SBS ion waves

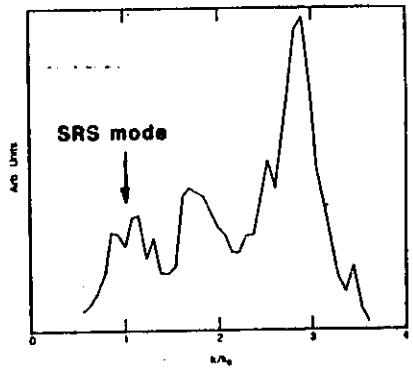


SBS ion waves disrupt the SRS phase matching requirements, causing SRS to collapse

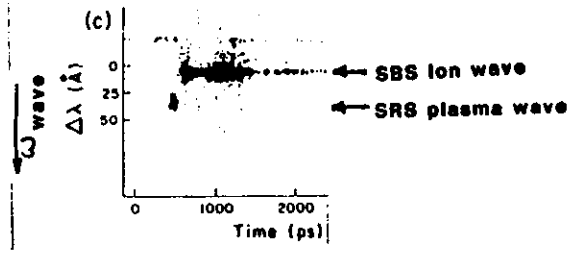

Private communication by H. A. Baldis

## Summary of 3-μm CH foil time-dependent behavior

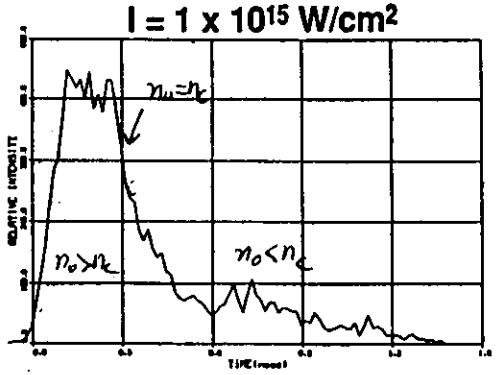


SBS signal ↑

Shot # 16100902

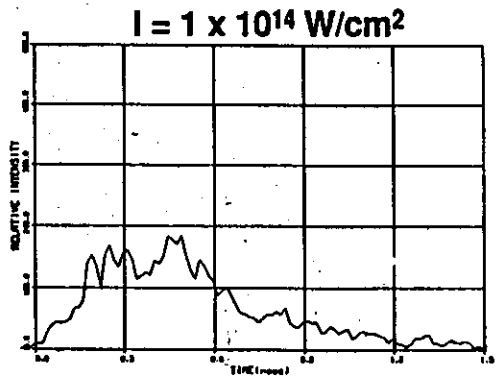


Shot # 16091809

$n_o < n_c$

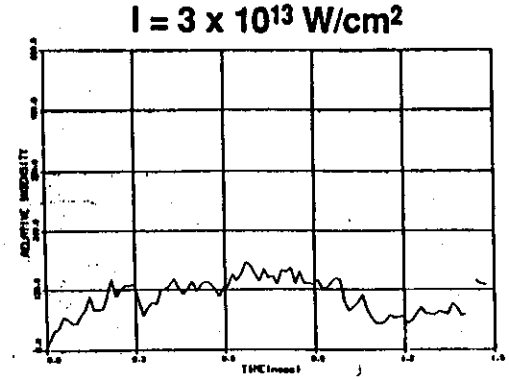


Shot # 16090508

$n_o < n_c$



Private communication by H. A. Baldis

SBS

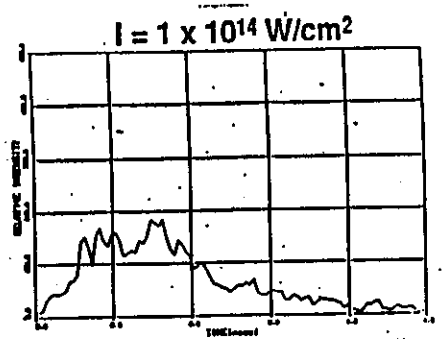


SRS

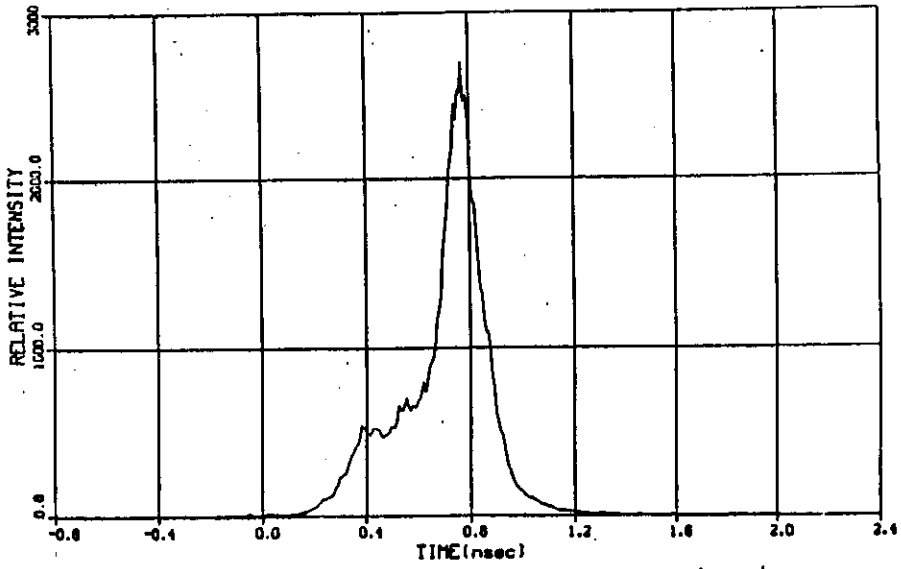


low density

SOS: 16082210505-1
X- 5.5952E+02(nm)

Private communication by [illegible] Baldis

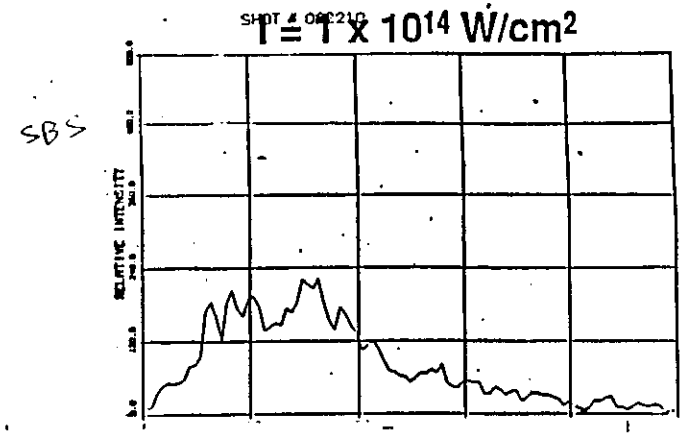


SBS

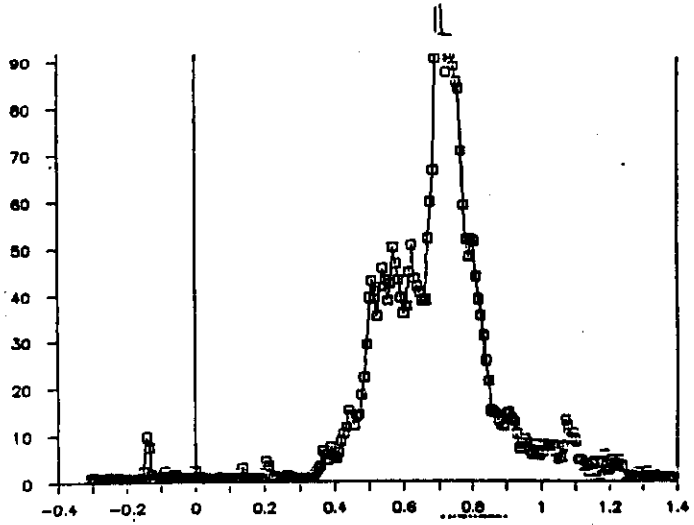


SRS

high density